ISSN 0038-0946, Solar System Research, 2017, Vol. 51, No. 5, pp. 347–361. © Pleiades Publishing, Inc., 2017.
Original Russian Text © E.E. Grigorenko, S.D. Shuvalov, H.V. Malova, V.Yu. Popov, V.N. Ermakov, E. Dubinin, L.M. Zelenyi, 2017, published in Astronomicheskii Vestnik, 2017, Vol. 51, No. 5, pp. 376–391.

Structure of the Current Sheets in the Near-Mars Magnetotail. Maven Observations[1]

E. E. Grigorenko[a, *], S. D. Shuvalov[a], H. V. Malova[a, b], V. Yu. Popov[a, c, d], V. N. Ermakov[a], E. Dubinin[e], and L. M. Zelenyi[a]

[a] *Space Research Institute of Russian Academy of Science, Moscow, Russia*
[b] *Scobeltsyn Nuclear Physics Institute of Lomonosov Moscow State University, Russia*
[c] *Physics Department of Lomonosov Moscow State University, Russia*
[d] *Higher School of Economics, National University, Moscow, Russia*
[e] *Max Planck Institute for Solar System Research, Göttingen, Germany*
**e-mail: elenagrigorenko2003@yandex.ru*

Received December 8, 2016

Abstract—During the last 15 years, the Current Sheets (CSs) have been intensively studied in the tail of the terrestrial magnetosphere, where protons are the dominated ion component. On the contrary, in the Martian magnetotail heavy ions (O^+ and O_2^+) usually dominate while the abundance of protons can be negligible. Hence it is interesting to study the spatial structure and plasma characteristics of such "oxygen" CSs. *MAVEN* spacecraft (s/c) currently operating on the Martian orbit with a unique set of scientific instruments allows observation of the magnetic field and three-dimensional distribution functions of various ion components and electrons with a high time resolution. In this paper, we analyse nine intervals of the CSs observed by *MAVEN* in the near-Mars tail at the distances from the planet ~1.5–1R_M, where R_M is the radius of Mars. We analyse the spatial structure of the CSs and estimate their thickness for different magnetic configurations and relative abundance of the heavy and light ions in the sheets. It is shown that, similarly to the CSs in the Earth's magnetotail, the thickness and complexity of the spatial structure of the Maritan CSs (i.e. the presence of embedded and / or peripheral current structures) depend on the magnetic configuration of the sheets, which, in turn, affects the fraction of the quasi-adiabatic particles in the CSs.

Keywords: Mars magnetosphere, current sheets, quasi-adiabatic ion dynamics

DOI: 10.1134/S0038094617050033

INTRODUCTION

Current sheets (CSs) are one of the most common plasma structures observed in space and laboratory plasmas. Mechanisms of self-organization and maintenance of quasi-equilibrium CS configurations, as well as the processes of energy accumulation and transformation are the important problems of plasma physics for many decades. The intense studies of the CSs in collisionless space plasma have shown that the presence of several ion populations with different masses and/or energies can significantly affect the structure and dynamics of the CSs, in particular, lead to the formation of embedded current configurations (e.g. Zelenyi et al., 2011 and references therein). The latter can become a source of free energy to excite various plasma instabilities in the CS, which, in turn, can result in a weakening or disruption of the CS and magnetic reconnection (e.g. Zelenyi et al., 2008; Pritchett, 2010; Grigorenko et al., 2014). The studies of the CSs in hot collisionless plasma of the Earth's magnetotail have shown that quite often the CSs represent the complex spatial structures either consisting of several embedded current layers or bifurcated (splitted) layers (e.g Runov et al., 2003; Zelenyi et al., 2006). Multipoint Cluster observations allowing the separation of spatial and temporal effects proved that complex current configurations are indeed spatial structures, the current in which is carried by various plasma components: electrons, protons, heavy ions. The complex quasi- and nonadiabatic dynamics of different plasma populations in the CS define the abundance of trapped, quasi-trapped and transit particles, which, in turn, self-consistently affect the magnetic structure and the current density distribution in the CSs (Zelenyi et al., 2016 and references therein).

Another interesting feature of the CS observed in the Earth magnetotail is the presence of the shear component of the magnetic field which is either parallel or antiparallel to the direction of the electric current in the sheet. At least three basic types of the spatial dis-

[1] The article was translated by the authors.

tribution of the shear magnetic field across the CS were detected (see e.g. Malova et al., 2015 and references therein). The first type is the so-called antisymmetric distribution when the absolute value of the shear field is amplified at the edges of the sheet and it changes its sign at the neutral plane of the CS. This distribution of the shear magnetic field is often observed in the vicinity of the magnetic X-line and is associated with the formation of Hall currents flowing from the magnetic reconnection region along the Earth-Sun line (e.g. Eastwood et al., 2007).

The second type of the shear field distribution is the symmetrical or "bell-shaped" distribution when the absolute value of this field is amplified at the neutral plane of the CS and decreases outside the CS (e.g. Rong et al., 2011; Grigorenko et al., 2015). Such distribution of the shear magnetic field is often observed in closed plasmoid-like structures (e.g. Slavin et al., 1989; Grigorenko et al., 2013). And, finally, the third type of distribution is characterized by a quasi-constant shear field component across the CS, which magnitude does not depend on the distance from the neutral plane.

Initially, it was believed that a shear magnetic field appears in the Earth's magnetotail as a result of the penetration of the interplanetary magnetic field (IMF) (see e.g. Fairfield, 1979, Kaumaz et al., 1994). However, the antisymmetric and symmetric spatial distributions of this field in the CS cannot be explained in the frame of the IMF penetration (e.g. Grigorenko et al., 2015). The amplification of a shear field at the neutral plane of the CS or at the edges of the CS, in comparison with the "background" value, can be due to the internal dynamics of the CS.

In the tail of the induced Martian magnetosphere the CSs are also often observed. Observations of the CSs on the night side of Mars were made at various distances from the planet from ~1000 km, where the effects of magnetic anomalies are small (see e.g. Dubinin et al., 1991; Acuña et al., 1999), and up to distances ~400 km , where the effects of crustal magnetic fields can be significant. These observations show that, even at low altitudes, the induced magnetic fields still play a significant role in the formation of the current structures (Ferguson et al., 2005).

Unlike in the Earth magnetotail the plasma composition in the Martian tail is more variable and interesting. In the Earth's tail, the main plasma components are electrons and protons, and the fraction of heavy ions (He^+, He^{2+}, O^+ ions) is relatively small and does not exceed 20% (e.g. Kronberg et al., 2014 and references therein). Nevertheless, even such a small fraction of heavy ions can significantly affect the structure of the CS, contributing to its thickening and/or to the formation of embedded current configurations (e.g. Zelenyi et al., 2006; Petrukovich et al., 2011). In contrast, in the Martian tail plasma, heavy (oxygen) ions are often the dominant component. In a statistical study of the CSs observed at low altitudes by the Mars Global Surveyor (MGS), it was shown that the main current carriers in the CS can be ions (Halekas et al., 2006). Thus, the "in situ" spacecraft studies of the structure and dynamics of CS with different mass composition and testing of the existing models of the multicomponent CSs represent a great interest.

Unfortunately, until the present time, the regular observations in Martian magnetotail with a good set of plasma instruments were not carried out. On the *Mars Express* spacecraft, which has been operating for many years on the orbit of Mars, there is no magnetometer, so that it is impossible to study the magnetic structure of the CSs. Only in 2014 the *MAVEN* spacecraft started to operate on the Mars orbit with a full set of plasma devices, which allow the detailed studies of the plasma composition, energy spectra, and three-dimensional distribution functions of charged particles with a good time resolution.

This paper presents a study of nine crossings of the CS in the near-tail region of the Martiam magnetosphere by *MAVEN* s/c on 04.12.2014. The observed spatial distributions of the current density are compared with the results of model simulations. We showed that the mechanisms of the formation of current density spatial distributions revealed for the Earth's magnetotail CS are also relevant for the Martian tail. In particular, it is revealed that the thickness and complexity of the CS structure in the Martian tail (the presence of embedded structures) depend on the magnetic configuration of the sheet, which, in turn, defines the fraction of quasi-adiabatic particles in the CS.

The content of the paper is as follows. In the section "Used data" we will describe the spacecraft data used for the CS analysis; In the section "Observations of the CS in the Martian magnetotail" an example of the CS crossing is presented along with the observed magnetic and plasma characteristics. In this section we also describe the methods used for the analysis of the CSs. In the section "Characteristics of the CS in the Martian magnetotail", the characteristics of the CS observed in nine CS crossings analysed in this paper are generalized. The comparison of the observed CS structures with the model simulations are made in the section "Comparison of the observed characteristics of the CS with model simulations". The last section presents the discussion of the results, conclusions and open questions.

USED DATA

In this paper, we use the MAVEN (Mars Atmosphere and Volatile EvolutioN Mission) observations in the near-Mars tail region at distances from the planet $-1.5R_M < X_{MSO} < -1R_M$ in December 2014. *MAVEN* s/c was launched in November 2013 and entered the orbit around Mars in September 2014. The

orbit period is ~5 hours. The mission's scientific goals and instrumentation are described in detail in the paper by Jakosky et al., 2015.

For the CS analysis we used the magnetic field observations by the MAG magnetometer (Connerney et al., 2015) and ion moments obtained by the STATIC ion spectrometer (McFadden et al., 2015).

Everywhere in the paper, the MSO (Mars Solar Orbital) coordinate system is used. In this coordinate system the X axis is directed to Mars along the Mars-Sun line, the Z axis is perpendicular to the plane of Mars orbit and the Y axis is complementary to the right-handed triplet of vectors, being antiparallel to the Martian orbital velocity vector.

OBSERVATION OF THE CS IN THE MARTIAN MAGNETOTAIL

Figure 1 shows an example of the orbit of the MAVEN s/c in the (XY) and (XZ) planes. Red colour shows the segment of the orbit crossing the Near-Mars CS. Figure 2 shows an example of the CS observation on 04.12.2014 in 14:44–14:53 UT. The figure shows from top to bottom: the time profiles of three components of the magnetic field; X-components of the velocity of H^+ ions (shown in black), O^+ (shown in red) and O_2^+ (shown in green); the parallel and perpendicular components of ion velocity, density, and temperature. As can be seen from the figure, the change in the sign of the B_X-component of the magnetic field, indicating the CS crossing takes place at 14:48–14:50 UT (the grey shaded interval in Fig. 2). It is seen from the figure that in the vicinity of the neutral plane (where $B_X = 0$) an increase in the perpendicular velocity of H^+ ions is observed, while outside the CS (in the region with $|B_X| > 0$) protons are moving mainly along the magnetic field lines with V_{PAR} in several times larger than the local Alfven velocity, V_A (the time profile of V_A is shown by the blue line).

Accelerated ion fluxes moved from Mars tailward (the V_X component was negative for the entire time interval). The density of heavy ions during the interval of interest was high (>10 cm^{-3}) and exceeded the proton density. The ratio of the proton density to the densities of heavy ions in a given CS crossing was $n_H^+/n_O^+ \sim 0.15 n_H^+/n_{O_2}^+ \sim 0.06$, i.e. heavy ions represent the dominated ion component in the CS. The temperatures of all the ion components were approximately the same ~10 eV.

To analyse the spatial structure of the CS, we used the Minimum Variance Analysis technique (MVA) (Sönnerup and Scheible, 1998), assuming that *MAVEN* crossed a plane and quasi-stationary current structure. As can be seen from Fig. 2, during the CS crossing the reversal of the B_X field was approximately monotonic,

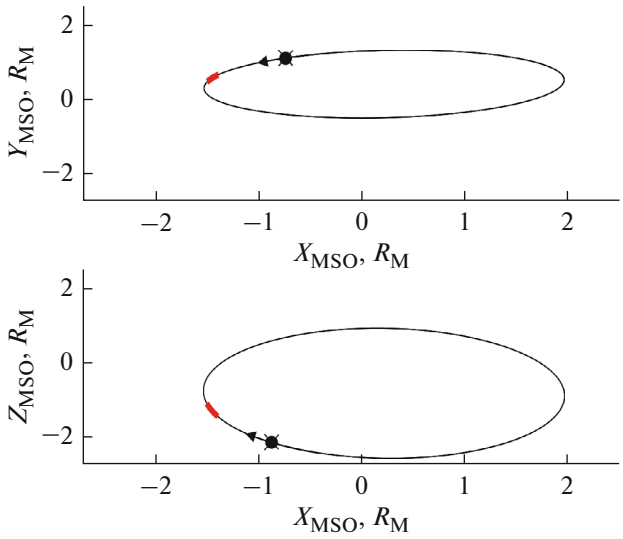

Fig. 1. An example of the MAVEN orbit on 04.12.2014 at 14: 00–19: 00 UT plotted in the (XY) MSO and (XZ) MSO planes. The intervals of the CSs crossings are shown by red colour.

so that one may assume that the B_X reversal is a result of the crossing of spatial current structure.

Applying the MVA analysis to the time interval at 14:46–14:51 UT we obtain the following direction of the normal to the CS: $N = [-0.5, -0.1, 0.8]_{MSO}$ and of the maximum magnetic field variation $MAX = [0.8, -0.2, 0.5]_{MSO}$. Thus, the directions of the vectors obtained from the MVA analysis are close to the directions of the axes of the MSO system. The CS is oriented almost horizontally in the plane of the ecliptic with a slope in the (XZ) plane ~ 17°.

Taking into account the assumptions on 1D planar CS geometry we estimate the value of the current density measured at each time moment t_i during the CS crossing as: $J_i \sim \Delta B^i_{MAX}/l_N$, where $\Delta B^i_{MAX} = B^i_{MAX} - B^{i-1}_{MAX}$, $l_{Ni} = t_i V_N$ and V_N is the component of the average ion velocity perpendicular to the CS plane corrected for the spacecraft velocity. Then the thickness of the CS, L (i.e. the spatial scale of the current layer along the N) can be estimated as $L = \int_{t1}^{t2} V_N dt$, where $\Delta t = t_2 - t_1$ is the time interval of the B_{MAX} reversal. The current in the CS is parallel or antiparallel to the direction of the medium variation of the magnetic field B_{MID}.

Figure 3 shows the spatial profiles of the magnetic field component $B_{MAX}(l_N)$ reconstructed along the normal N to the CS plane, the spatial profile of the current density $J_{MID}(l_N)$, as well as the hodographs of the magnetic field components $B_{MAX}(B_N)$ and $B_{MAX}(B_{MID})$. From the hodographs of the magnetic field, it is seen that at the neutral plane of the CS

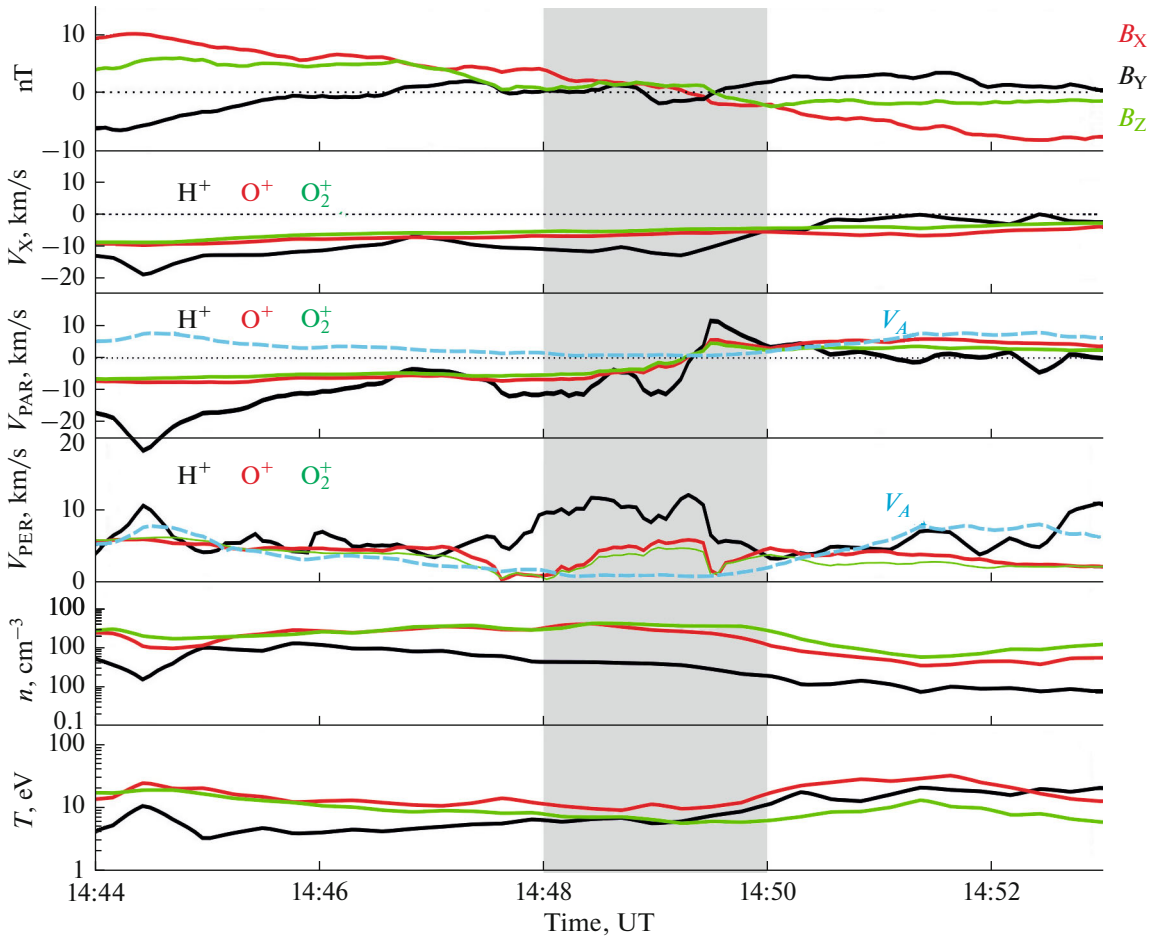

Fig. 2. Plasma characteristics observed by MAVEN during the CS crossing at 14:44–14:53 UT. The CS interval is shaded by grey. From top to bottom: the time profiles of three components of the magnetic field, the *X*-component, parallel and perpendicular velocities, density and temperatures of H^+, O^+, and O_2^+ ions. The time profile of the local Alfven velocity is shown by blue colour.

(where $B_{MAX} = 0$) the normal component of the magnetic field is $B_N = 0$, but there is a small nonzero shear magnetic field $B_{MID} \sim 3.0$ nT directed parallel to the electric current in the sheet.

In the spatial distribution of the current density $J_{MID}(l_N)$, a narrow peak with the current density at this peak is ~13 nA/m^2 is observed. The narrow current layer is embedded in a thicker layer (shaded in grey), whose total thickness is ~300 km. The observed variations in the current density J_{MID} at large $|l_N|$ are possibly related to some temporal variations of $B_{MAX}(t)$.

Figure 4 shows the dependences of the ion densities n_H^+, n_O^+, $n_{O_2}^+$ and the ratios of densities n_H^+/n_O^+ and $n_H^+/n_{O_2}^+$, as well as the ion β_{ion} calculated as $\beta_{ion} = k(n_H^+T_H^+ + n_O^+T_O^+ + n_{O_2}^+T_{O_2}^+)/(8\pi B^2)$ versus the value of B_{MAX}. In a simple 1D CS model the value of $|B_{MAX}|$ shows the proximity of the spacecraft to the neutral plane of the CS (where $B_{MAX} = 0$). Thus, Fig. 4 shows the spatial distribution of ion characteristics across the CS.

It can be seen from the figure that in the proton density distribution a pronounced asymmetry is observed: the density increases toward the positive values of B_{MAX}. As it was shown above at the neutral plane of the CS some nonzero component of the shear magnetic field exists (see the hodograph $B_{MAX}(B_{MID})$ in Fig. 3). In the presence of such a "bell-shaped" spatial distribution of the shear field across the CS, there is an asymmetry in the reflection/refraction of the quasi-adiabatic ions during their interaction with the sheet, which leads to the appearance of the north-south asymmetry in the ion density distribution. In the presence of positive shear magnetic field components near the neutral plane, these kinetic effects lead to some excess of ions injected towards the positive B_{MAX} hemisphere and to the corresponding asymmetry in the ion density distribution (Grigorenko et al., 2013; Grigorenko et al., 2015; Malova et al., 2015). The similar but smaller asymmetry in density distribution is also observed for O^+ ions: the maximum of density is shifted to the positive B_{MAX} values. This asymmetry, however, is not

observed in the distributions of heavier ions, which may be due to their larger gyroradius exceeding the characteristic spatial scale of the CS.

From Fig. 4 it is also seen that in this CS crossing heavy ions O^+ and O_2^+ dominated. Indeed, at the neutral plane of the CS the ratio $n_H^+/n_O^+ \sim 0.1$, and $n_H^+/n_{O_2}^+$ was even smaller. Ion β at the neutral plane was ~ 70.0. In contrast to the CS, in the Earth's magnetotail, where high values of the plasma pressure are due to high ion temperatures, the high ion pressure observed in the Martian CS is due to the high ion densities. The temperatures of the ion components at the centre of the CS were ≤10 eV.

In order to find out which ion population contributes to the observed current density in the CS, we plotted in Fig. 5 the dependences (J_{MID}, J_{ion}) for each time moment during the CS crossing, where J_{MID} is the value of the current density, estimated from the magnetic field observations and J_{ion} is the value of the net current carried by a given ion component and calculated as $J_{ion} = qnV_{MID}$, where q, n and V_{MID} are charge, density and velocity along the MID direction of a given ion component respectively. It is seen that the best correspondence between the J_{MID} and J_{ion} values is observed for the proton population. In other words, protons provide the main contribution to the observed current density in this CS crossing. Perhaps a thin and intense CS with a characteristic thickness of the order of the gyroradius of thermal protons (see Fig. 3) was created by a proton population, whereas heavier ions could contribute to the thicker and less intense layer surrounding the thin embedded proton layer.

CHARACTERISTICS OF THE CS IN THE MARTIAN MAGNETOTAIL

The analysis of the CS and plasma characteristics, presented in the previous section, was applied to other eight intervals of the CSs observed by *MAVEN* s/c. The analysed CS intervals and their characteristics are presented in the table.

Figure 6 shows the spatial profiles of $B_{MAX}(l_N)$, $J_{MID}(l_N)$, and $B_{MAX}(B_N)$, $B_{MAX}(B_{MID})$ in the format similar to the format of Fig.3. Nine CS from our database were divided into three groups (correspondingly, three columns in Fig. 6) according to their magnetic configurations.

The first group (the left column) includes CS with small normal and shear components of the magnetic field: $B_N/B_0 \le 0.1$, $B_{MID}/B_0 \le 0.1$, where B_0 is the value of the magnetic field outside the CS. In this group besides the CS interval considered in the previous section there are two intervals at 10:25–10:28 UT and at 10:32:30–10:33:40 UT. In all three crossings there are thin and intense CSs embedded in thicker and less intense current layers. The total thickness of the thin CSs varied from ~200 km (at 10:25–10:28 UT) to ~100 km

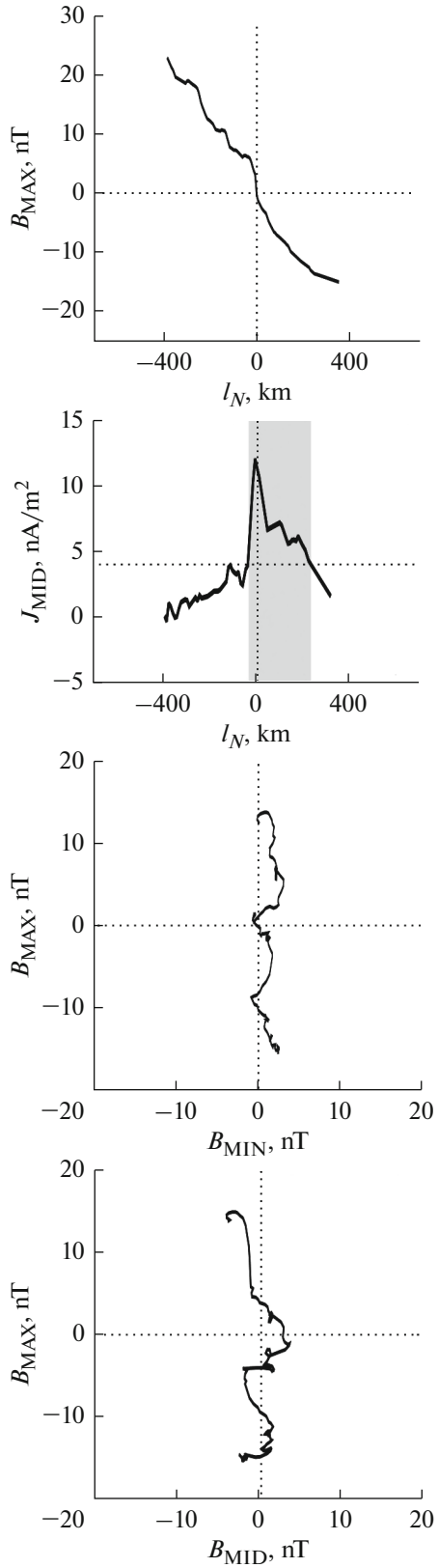

Fig. 3. The results of the analysis of the CS structure observed at 14: 44–14: 53 UT. From top to bottom: the spatial profiles of B_{MAX} (l_N); $J_{MID}(l_N)$ and the hodographs of the magnetic field (B_{MAX}, B_{MIN}) and (B_{MAX}, B_{MID}).

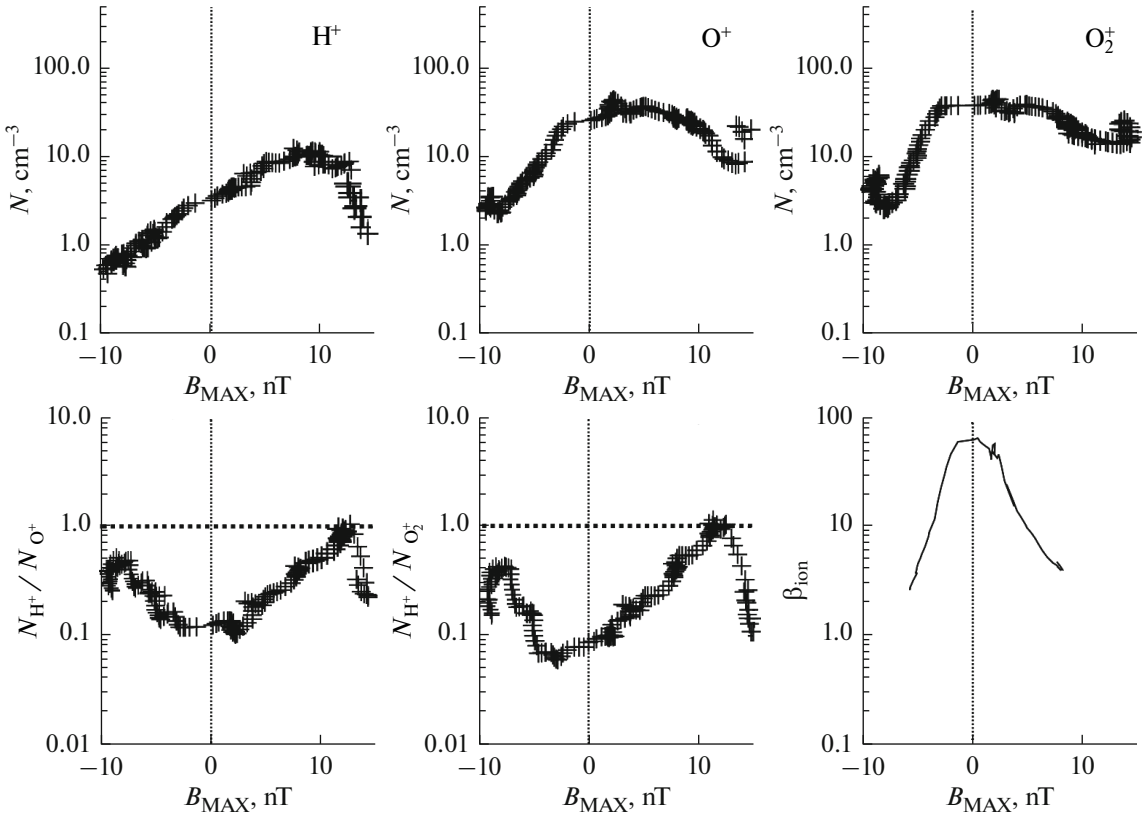

Fig. 4. The upper row: the dependences of density of H^+, O^+, and O_2^+ ions on the B_{MAX}, $N(B_{MAX})$. The bottom row: the dependencies of $N_H^+/N_O^+(B_{MAX})$ and $N_H^+/N_{O_2}^+(B_{MAX})$ and ion beta $\beta(B_{MAX})$.

(at 10:32:30–10:33:40 UT). In the latter case, the current density in a thin layer reached 20 nA /m^2. The proton temperature at this crossing was only 4 eV (see Table 1), the magnetic field value at the neutral plane was ~1 nT due to the presence of a weak shear field and, thus, the gyroradius of the thermal protons was ~280 km, i.e. exceeded the thickness of a thin intense layer. This indicates that the current in this layer can be carried by electrons.

Indeed, Fig. 7 shows the dependencies (J_{MID}, J_{ion}) observed at these three CS crossings (shown by the same colours as the spatial profiles of the current density in Fig. 6). The format of Fig. 7 is similar to the format of Fig. 5. It is seen that in two CSs, one of which was considered in the previous section, and at the CS crossing observed at 10:25–10:28 UT, protons most likely were the main current carried plasma component. In a very thin CS, observed at 10:32:30–10:33:40 UT, the current can be carried by electrons since for this interval no good correspondence between the net current of any ion component and the J_{MID} was observed.

In the second column of Fig. 6, two cases of the CSs with a significant normal component of the magnetic field ($B_N/B_0 \geq 0.5$) are presented. In these crossings the shear component of the magnetic field was small: $B_{MID}/B_0 \sim 0.1$. These CSs (at 01:29–01:34 UT and at 01:41–01:42 UT) are characterized by a lower current density and larger thickness. This is clearly observed for the CS crossing at 01:29–01:34 UT, in which the value of the B_N was the largest (the corresponding profile is shown by red colour in Fig. 6). The total thickness of this CS reached 500 km. From Fig. 8 (the same format as in Fig. 7), it can be seen that in both CSs heavy ions O^+ and O_2^+ provided the main contribution to the observed current density. The CS observed at 01:41–01:42 UT (the blue profile in Fig. 6) has smaller thickness (~250 km) although the normal component of the magnetic field was significant: $B_N/B_0 \sim 0.8$. Contrary to the previous two CSs from this group, in this CS protons dominated and the abundance of heavy ions was insignificant so that $n_H^+/n_O^+ = n_H^+/n_{O_2}^+ \sim 2.0$. It should also be noted that in this crossing the absolute value of the magnetic field $|B|$ was large at the neutral plane and the population of thermal protons was adiabatic. Indeed, for thermal protons the parameter of adiabaticity $\kappa(E) = \frac{B_{CS}}{B_0}\sqrt{\frac{L}{\rho(E)}}$ (Büchner and Zelenyi, 1989)

exceeded 1.0 (here L is the thickness of the CS, B_{CS} is the minimum value of the magnetic field observed at the neutral plane, $\rho(E)$ is the gyroradius of the ion with energy E and B_0 is the magnetic field outside the CS. For heavy O^+ and O_2^+ ions the condition $\kappa \le 1.0$ was fulfilled for temperatures > 40 eV and 30 eV respectively. Since in this CS interval the temperatures of the O^+ and O_2^+ ions were ~50 eV, then one may consider these populations to be quasi-adiabatic. These ions can provide the major contribution to the observed current density.

And, finally, in the right column in Fig. 6 the CS intervals with significant shear component (B_{MID}) of the magnetic field and with small normal component (B_N) are presented: $B_{MID}/B_0 \ge 0.3$, $B_N/B_0 \le 0.2$. In three of the four CS intervals, the spatial profile of the shear field had a "bell-like" shape, i.e. the value of $|B_{MID}|$ increases near the neutral plane and decreases outside the CS. The thickness of these CSs was ~200–400 km. For all CSs from this group, a particularly good agreement between the current density estimated from the magnetic field observations and the net current density carried by heavy ions was observed (see Fig. 9, the format is similar to that in Fig. 8). For example, in the CS observed at 05:58–06:02 UT, thermal protons (~20 eV) were practically magnetized ($\kappa >$ 1.0 up to proton energies ~40 eV). For heavy ions (the predominant population in this crossing), having temperatures T_O^+ ~125 eV and $T_{O_2}^+$ ~ 110 eV the condition $\kappa < 1.0$ is fulfilled already for energies ~ several eV. Thus, heavy ions could contribute to the current in a given CS crossing. The similar characteristics were observed in the other CS crossings from this group: heavy ions were the dominated ion population and contrary to protons they experienced quasi-adiabatic dynamics in the CSs.

Thus, in the nine CS intervals analysed in this paper various magnetic configurations and plasma characteristics were observed during a few successive flybys of the Martian tail region. In some CSs, a nonzero shear component of the magnetic field with the "bell-shaped" spatial profile similar to the one observed in the Earth's magnetotail was detected. The ion composition in the CSs also changed significantly. As can be seen from the Table, the ratio of n_H^+/n_O^+ and $n_H^+/n_{O_2}^+$ ranged from ~0.06 to ~2.0. In the majority of the analysed CSs heavy ions were the dominant component since their densities were several times higher than the density of protons. As a result in many CSs heavy ions provided the major contribution to the observed current density in the sheets. In the next section we compare the observed characteristics of the CSs with model simulations.

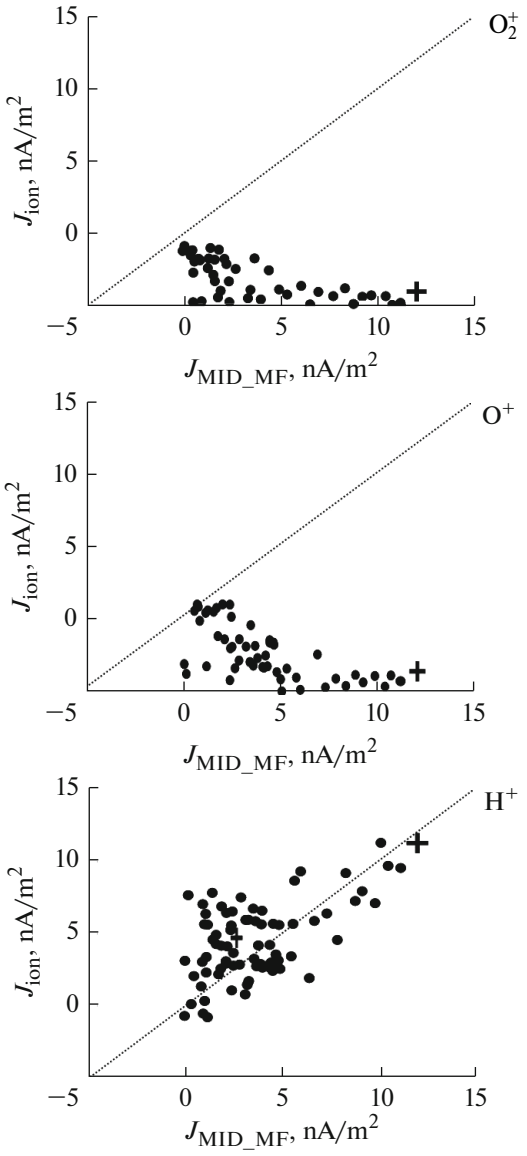

Fig. 5. From top to bottom: the comparison of the current density, calculated from the magnetic field variations observed by *MAVEN* (J_{MID_MF}) and the net current densities produced by O_2^+, O^+, and H^+ ions.

COMPARISON OF THE OBSERVED CHARACTERISTICS OF THE CS WITH MODEL SIMULATIONS

To describe the CS in the Martian magnetotail the hybrid self-consistent model is constructed. In the model the quasi-adiabatic dynamics of heavy ions and the presence of nonzero shear magnetic component are taken into account. The basic principles of the model are described in Zelenyi et al., 2004; 2006; 2016). In the model the following assumptions are made:

(1) The CS is supported by plasma flows coming from the opposite lobes of the tail;

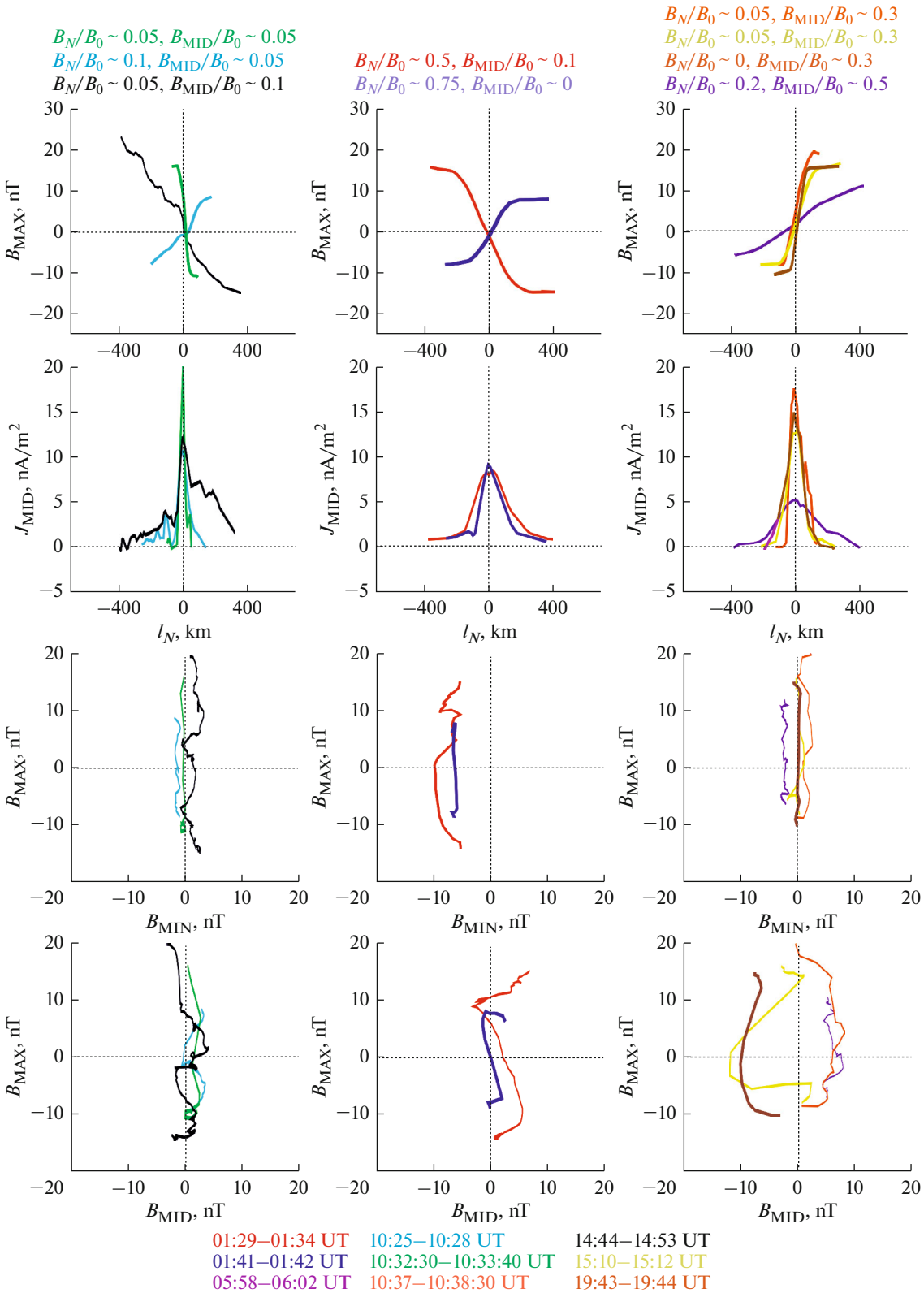

Fig. 6. The results of the analysis of the CSs structures observed in nine crossings by *MAVEN* s/c on 04.12.2014. The CSs were divided into three groups (three columns in the Figure) according to the values of ratio of the normal (B_N) and shear (B_{MID}) magnetic field components at the neutral plane to the value of the magnetic field outside the CS (B_0). The values of B_N/B_0 and B_{MID}/B_0 are shown above each column. In each column (the CS group) from top to bottom are shown: the spatial profile of the B_{MAX} field versus the coordinate l_N along the normal to the CS; the spatial profile of the electric current density $J_{MID}(l_N)$; the hodographs of (B_{MAX}, B_{MIN}) and (B_{MAX}, B_{MID}). In the bottom of the Figure we display the time intervals of a particular CS observation shown by the same colour as the corresponding spatial profiles and hodographs.

(2) the thickness of the CS along the normal N is much less than the CS scales in the directions along the direction of electric current (MID) and in the direction tangential to the CS plane and perpendicular to the current direction (MAX). Thus, all characteristics depend on the transverse coordinate along N;

(3) the normal and shear components of the magnetic field are assumed to be constant;

(4) the plasma consists of magnetized electrons and of quasi-adiabatic ($\kappa \le 1.0$, Büchner and Zelenyi, 1989) ions (H^+, O^+, O_2^+);

(5) the quasineutrality is conserved in the system due to the fulfilment of the Boltzmann approximation for electrons, which allows taking into account the electrostatic effects.

For the simulations the following average characteristics of the CS plasma were used (see Fig. 6 and Table 1): $B_N/B_0 = 0.1$–0.5; $B_{MID}/B_0 = 0.1$–0.5; n_H^+/n_O^+ and $n_H^+/n_{O_2}^+ = 0.5$; $V_{TO}/V_D \sim 1.0$, where V_{TO} is the thermal velocity of oxygen ions, and V_D is their velocity along the magnetic field lines outside the CS; $\rho_O^+/L \sim 1.0$, where L is the initial assumed thickness of the CS and $\rho_O^+ \sim 400$ km is the gyroradius of thermal oxygen ions in the CS. It was assumed that outside the CS the magnetic field $B_0 = 20$ nT and plasma density is $n_0 = 10$ cm^{-3}.

The system of Vlasov-Maxwell equations was solved numerically and the self-consistent spatial profiles of the magnetic field, current density and plasma density in the N direction (l_N) were found. Figure 10 shows the magnetic field profiles (left plot) and the current density profile (middle plot) obtained from the model by using the constant value of the normal component of the magnetic field in the CS $B_N = 0.1B_0$ and by using different values of the shear magnetic field B_{MID}/B_0 ranged from 0.0 to 0.5. It is seen that with the increase of the shear filed (B_{MID}/B_0 increase) the value of the current density at the neutral plane (at $l_N = 0$) decreases and the thickness of the CS increases. For small values of the shear field (the corresponding profiles are shown in black and red), a narrow embedded current layer can be seen near the neutral plane of the CS. This layer can be interpreted as a drift electron current (Zelenyi et al., 2004), which decreases significantly with the increase of the shear magnetic field. Electron currents can be important only for a zero shear component and for a small value of the normal magnetic field. As the |B| at the neutral plane increases the contribution of electron currents to the total current density becomes substantially less than the contribution from ion currents.

Malova et al., 2012; 2015 showed that in the presence of magnetic shear, a geometric effect takes place: ions touch the neutral plane earlier than in the case of zero shear field. This results in inclination of the

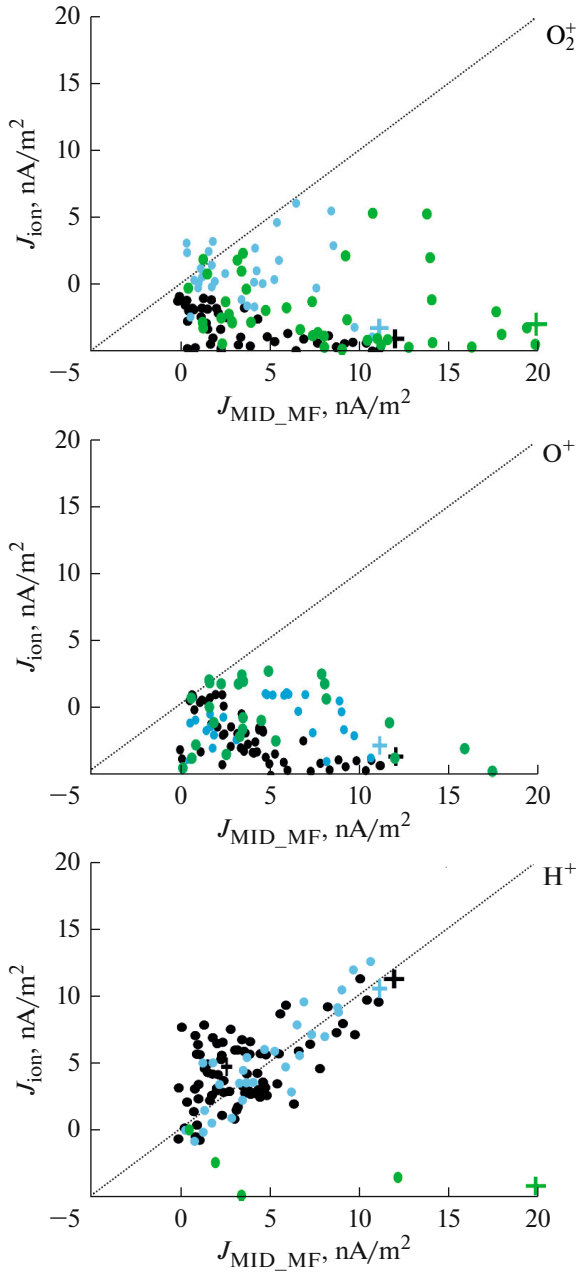

Fig. 7. The scatterplots of the current density J_{MID_MF}, calculated from the magnetic field observations versus the net current density produced by O_2^+, O^+, and H^+ ions for the CS from the first group (from the left column of Fig. 6), which are characterized by small values of B_N and B_{MID} at the neutral plane. The color of the scatterplots is the same as the colour of corresponding CS profiles in Fig. 6.

meandering orbits relative to the neutral plane and thickening of the CS. In turn, the increase in the CS thickness leads to the increase of the radius of curvature of the magnetic field lines and to decrease of plasma pressure gradients, and to a corresponding decrease of the drift currents (gradient, curvature and others). Thus, the contribution of electron currents in

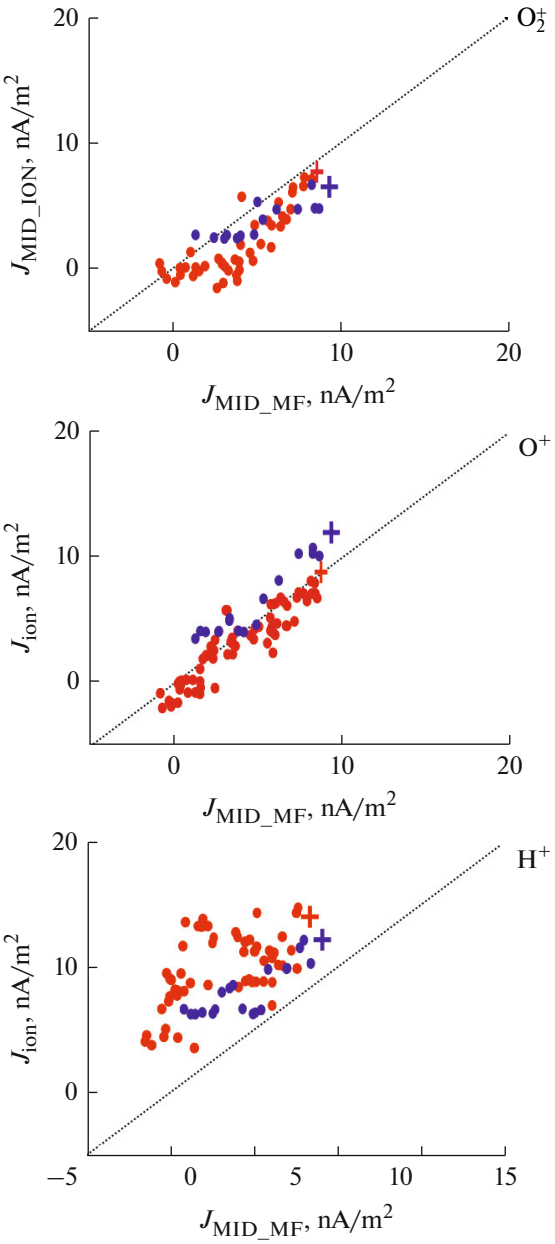

Fig. 8. The format is similar to Fig. 7, the data are presented for the CS from the second group (the central column in Fig. 6), which are characterized by the large value of the B_N and small value of a shear magnetic field B_{MID}.

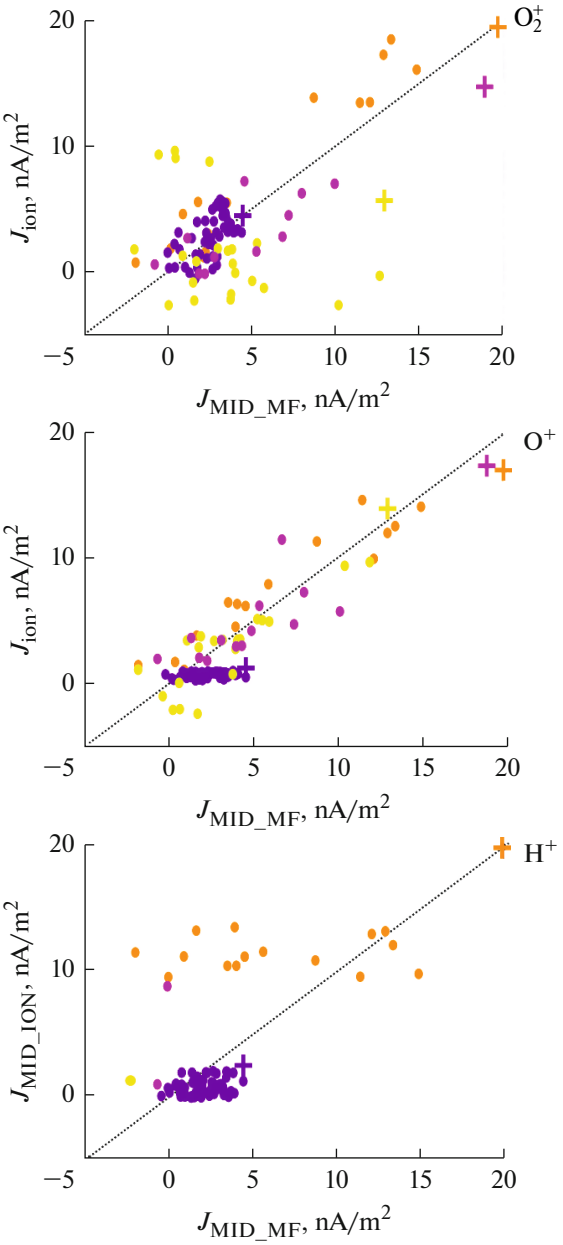

Fig. 9. The format is similar to that in Figs. 7, 8. The data are presented for the CSs from the third group (right column in Fig 6), which are characterized by the large values of B_N and B_{MID}.

the CS configuration with nonzero shear field $B_{MID}/B_0 >$ 0.2 can be negligibly small.

With the increase of the normal component of the magnetic field in the CS $B_N = 0.3B_0$ and for the same values of the shear field the thickness of the CS becomes even larger and the current density becomes smaller (see Fig. 11, made as in the same format as in Fig. 10).

On the right plot of Fig. 10 the model current density profiles $J_{MID}(l_N)$, calculated for the plasma and magnetic field parameters observed in three CS crossings from our data base are presented:

(1) at 10:25–10:28 UT with $B_N/B_0 = 0.1$; $B_{MID}/B_0 = 0.05$ (the observed profile is shown by the light grey solid line and the corresponding model profile is shown by the solid black line);

(2) at 01:29–01:34 UT with $B_N/B_0 = 0.5$; $B_{MID}/B_0 = 0.1$ (the observed profile is shown by the dark grey dashed line and the corresponding model profile is shown by the black dashed line);

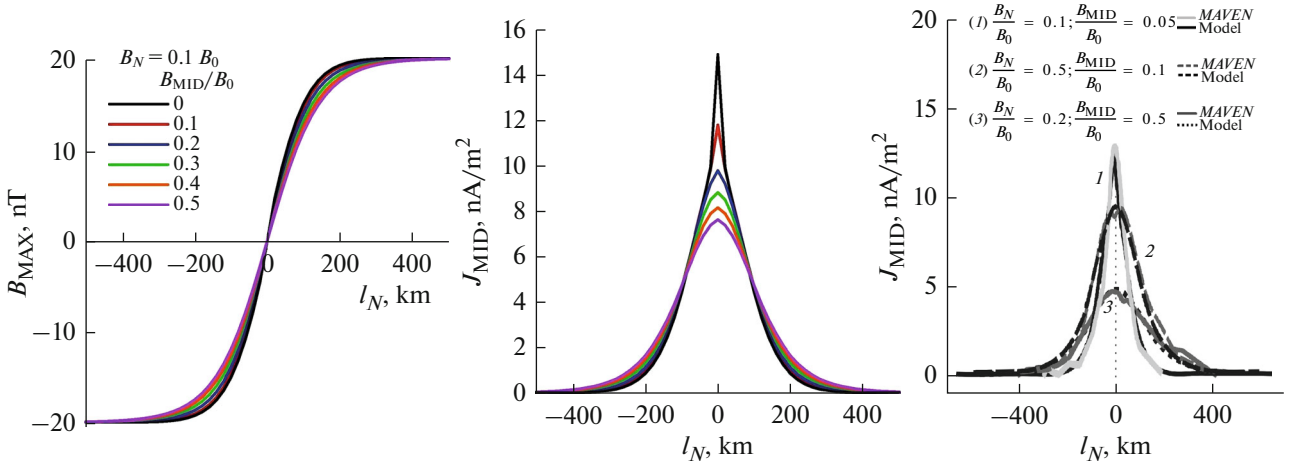

Fig. 10. The model spatial distribution profiles of the magnetic field component along the direction of the maximum variation of the B_{MAX} field (the left plot) and the current density J_{MID} (the middle plot) along the normal to the CS (l_N). The model profiles are calculated for different values of the shear component (B_{MID}/B_0) and for a small value of the normal component of the magnetic field $B_N = 0.1B_0$. In the right plot the spatial profiles of the current density $J_{MID}(l_N)$, constructed from the magnetic field observations in the CS crossings at: (*1*) 10:25–10:28 UT; (*2*) 01:29–01:34 UT; (*3*) 05:58–06:02 UT and the corresponding model current density profiles calculated from the magnetic and plasma parameters observed by MAVEN in these crossings.

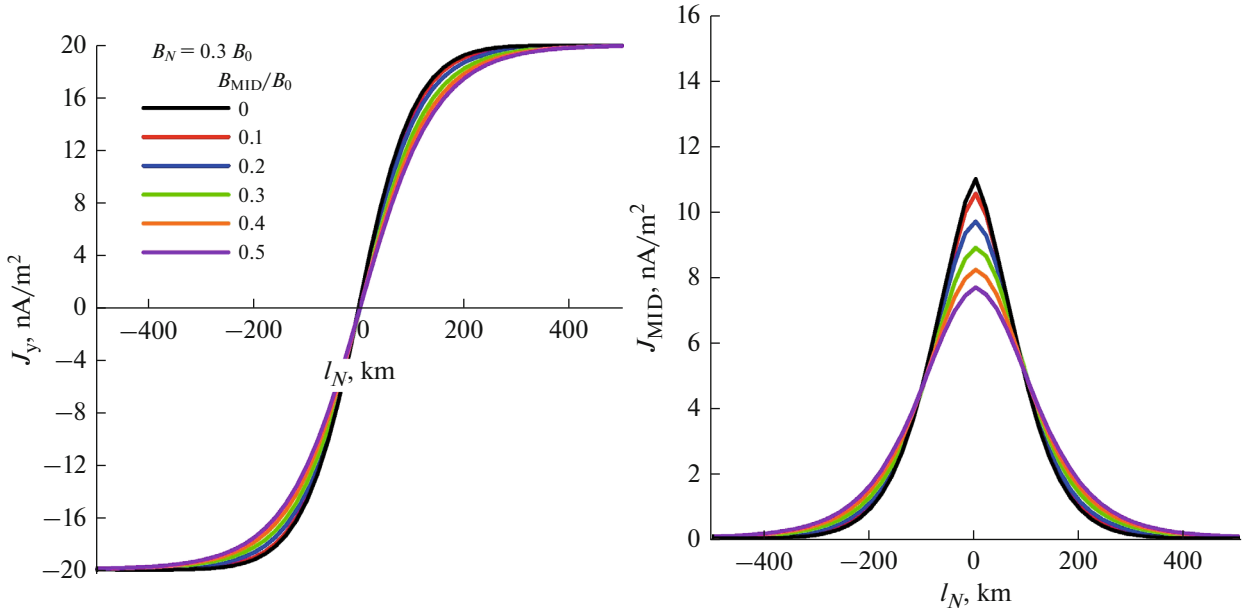

Fig. 11. The model spatial profiles of the $B_{MAX}(l_N)$ (the left plot) and $J_{MID}(l_N)$ (the right plot) obtained for the different values of the B_{MID}/B_0 and for a significant value of the normal component of the magnetic field at the neutral plane of the CS: $B_N = 0.3B_0$.

(3) at 05:58–06:02 UT with $B_N/B_0 = 0.2$; $B_{MID}/B_0 = 0.5$ (the observed current profile is shown by the solid dark grey line and the corresponding model profile is shown by the black dotted line).

It is seen that there is a good agreement between the current density profiles reconstructed from the MAVEN magnetic field observations and the model profiles calculated by use the plasma and magnetic characteristics observed by MAVEN in the corresponding time intervals. With an increase in the BN at the neutral plane, the thickness of the CS increases, and the current density decreases (see profiles "1" and "2"). This effect becomes more pronounced when the shear component of the magnetic field is increased (see profiles "2" and "3").

Thus, the simulation results are in qualitative agreement with the *MAVEN* observations. Indeed, in the case of the absence of the shear and normal mag-

Table 1. The list of the CS crossings by *MAVEN* s/c on 04.12.2014 and their plasma characteristics

Time Interval, UT	MVA Results	n_H^+/n_O^+	$n_H^+/n_{O_2}^+$	T_H^+, eV	T_O^+, eV	$T_{O_2}^+$, eV	β_{ion}
01:29–01:34	N = [–0.1, –0.3, 0.9] MID = [0.1, 0.9, 0.3] MAX = [0.98, –0.1, 0.1]	0.15	0.07	32.0	30.0	35.0	10.0
01:41–01:42	N = [0.0, 0.9, 0.4] MID = [0.8, 0.2, –0.5] MAX = [0.6, 0.3, 0.7]	2.2	1.7	47.0	37.0	56.0	4.0
05:59–06:02	N = [0.2,0 .2, 0.9] MID = [0.2, 0.9, –0.3] MAX = [0.9, –0.3, 0.1]	0.7	0.06	22.0	125.0	106.0	12.0
10:25–10:28	N = [–0.2, –0.2, 0.9] MID = [0.1, 0.96, 0.3] MAX = [0.97, –0.1, 0.2]	0.3	0.25	3.6	3.7	4.0	74.0
10:32:30–10:33:30	N = [–0.2, –0.5, 0.85] MID = [0.2, 0.8, 0.5] MAX = [0.95, –0.3, 0.1]	0.8	1.0	4.0	6.0	6.0	66.0
10:37–10:38:30	N = [0.2, 0.97, –0.1] MID = [–0.3, 0.1, 0.95] MAX = [0.9, –0.2, 0.3]	0.7	0.35	5.0	6.0	6.5	12.0
14:46–14:51	N = [–0.5, –0.1, 0.8] MID = [0.1, 0.98, 0.2] MAX = [0.8, –0.2, 0.5]	0.15	0.06	6.0	10.0	6.0	69.0
15:10–15:12	N = [0.1, 0.9, –0.4] MID = [–0.6, 0.4, 0.7] MAX = [0.8, 0.2, 0.6]	0.4	0.2	4.0	4.5	5.0	4.0
19:43–19:44	N = [0.2, –0.3, 0.9] MID = [–0.6, 0.7, 0.4] MAX = [0.7, 0.6, 0.2]	1.4	0.7	5.0	10.0	8.0	3.0

netic field component a thin intense CS is observed (see the green profile in the left column in Fig. 6) and electrons can contribute to this current. At somewhat larger values of a shear or normal component of the magnetic field at the neutral plane (black and blue profiles, respectively), the current density in the central thin layer decreases and the embedding feature is observed: a stronger and thinner layer is embedded in the weaker and thick CS created by quasi-trapped ions. As the shear component of the magnetic field increases, the current density in the layer decreases and the CS becomes thicker (see the middle column in Fig. 6). This effect is more pronounced if a significant normal component of the magnetic field is also present at the neutral plane (see, for example, the grey-green and violet profiles in the right column of Fig. 6). The thicknesses and current densities obtained in the model are also in a good agreement with the observations.

Our model does not take into account the fact that for the one and the same energy composition of plasma population, the number of trapped particles, whose contribution to the electric current is close to zero, increases with the normal component of the magnetic field B_N and as a result the current density decreases. This problem has not been fully investigated. Taking into account the relative fraction of the current carriers when the parameters of the system are changed is the subject of our further research. Also we plan to extend the statistics of the CS observations in the Martian tail in our next works.

DISCUSSION AND CONCLUSIONS

The analysis of nine CS crossings observed by *MAVEN* in the Martian magnetotail at the distances from the planet $-1.5R_M < X_{MSO} < -1R_M$ showed a variety of plasma and magnetic characteristics of the sheets. In the CSs from our data base proton density ranged from 1 to 100 cm^{-3} and the ratio of proton to O^+ density (n_H^+/n_O^+) ranged from 0.15 to 2.2, and the ratio $n_H^+/n_{O_2}^+$ ranged from 0.06 to 1.7. In the majority of cases the CSs were "oxygen" with $(n_H^+/n_O^+)_{mean} = 0.75$

and $(n_H^+/n_{O_2}^+)_{mean} = 0.5$, i.e. $n_H^+ < n_O^+ < n_{O_2}^+$. Thus, the ion composition of the CS in the Martian tail is significantly different from the ion composition observed in the CS of the Earth's magnetotail.

Nevertheless, theoretical models developed for terrestrial CSs based on the quasi-adiabatic ion dynamics showed a qualitative agreement between the model and observed spatial distributions of the magnetic field and the current density across the CS. The use of a hybrid model in which magnetized electrons and quasi-adiabatic protons, O^+ and O_2^+ ion components were taken into account showed that:

(1) the CS is a multiscale structure consisting of the embedded current layers with a thin and intense central layer created by electrons and/or by protons, which is embedded into a thicker and less intense CS created by heavy ions;

(2) in the thick CSs the main contribution to the electric current is provided by oxygen ions moving along quasi-adiabatic open orbits;

(3) the contribution of electrons to the total current density can be significant only for small values of the normal ($B_N/B_0 \le 0.1$) and shear ($B_{MID}/B_0 \le 0.2$) components of the magnetic field at the neutral plane;

(4) in the presence of a shear magnetic component, the thickness of the CS increases and the current density decreases.

The conclusions obtained from the theoretical simulations are basically confirmed by the *MAVEN* observations. Indeed, the presence of a thin intense CS embedded in a weaker and thicker layer is observed in the current density profiles presented in the left column in Fig. 6, i.e. for the magnetic configurations with small values of B_N and B_{MID}. Comparing the observed spatial profiles of the current density in the CSs without a shear field and with the nonzero shear component (the left and right columns in Fig. 6 respectively), one can see that with the increase of a shear component the current density decreases, the thickness of the CS increases, and the thin intense current layer disappears. The increase of the normal magnetic field component according to the model should lead to further thickening of the CS and weakening of the current density. This is exactly observed in CS at 01:29–01:34 UT (red profile in the middle column in Fig. 6). However, at another CS crossing from this group (at 01:41–01:42 UT), the CS is significantly thinner. It is worth to note that both crossings occurred within ~12 min interval, but the plasma characteristics of the CSs differed significantly from each other. In the first crossing in which the thick CS was observed heavy ions dominated over proton population: $n_H^+/n_O^+ = 0.15$ and $n_H^+/n_{O_2}^+ = 0.07$. Apparently, the large abundance of heavy ions influences on the CS thickness. We also found that in this CS interval heavy ions provided the major net contribution to the total electric current density (see Fig. 8). However, after 12 minutes, in the next CS crossing protons dominated: $n_H^+/n_O^+ = 2.2$ and $n_H^+/n_{O_2}^+ = 1.7$. This probably results in a reduction of the CS thickness due to smaller proton gyroradius. From Fig. 7 it is seen that in this CS the net proton current also contributes significantly to the observed total current density.

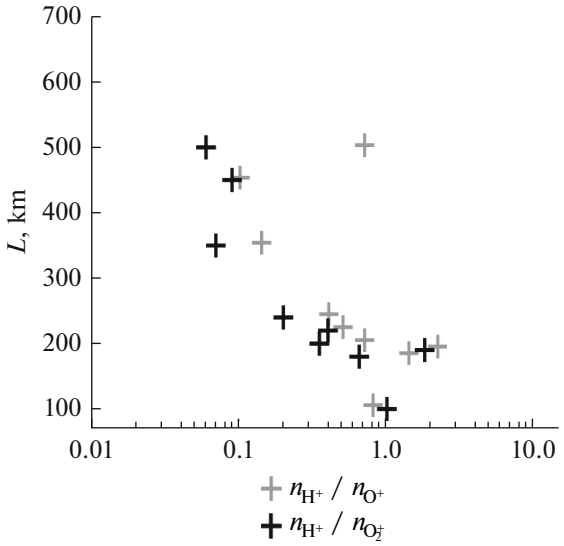

Fig. 12. The dependence of the CS thickness (L) on the value of the ratio of n_H^+/n_O^+, shown by grey crosses and on the ratio of $n_H^+/n_{O_2}^+$, shown by black crosses observed in nine CS analysed in the present paper.

There is also an agreement between the model and observed current carried plasma components. In the CS with a small BN and BMID the current is carried mainly by electrons (as in the CS observed at in 10: 32:30–10:33:40 UT, green profile in Fig. 6), and/or by protons (the CSs observed at 10:25–10:28 UT and 14:44–14:53 UT, the blue and black profiles in Fig. 6). In the other CSs with a significant BN and/or BMID component(s) the electric current was carried mainly by oxygen ions.

Besides the magnetic configuration, ion mass composition influences the structure of the CS. In the Earth's magnetotail the presence of multiscale embedded current configurations was explained by the formation of a thick current layer by heavy ions (Zelenyi et al., 2006). It is natural to assume that the similar effect takes place in the Martian CS because of the various ion composition.

Figure 12 shows the dependence of the CS total thickness (L) on the value of n_H^+/n_O^+ (shown by grey crosses) and on the value of $n_H^+/n_{O_2}^+$ (shown by black crosses). There is a tendency of L increase with the

decrease of n_H^+/n_O^+ or $n_H^+/n_{O_2}^+$, i.e. with the increase of relative density of heavy ions. Thus, the observed features of the CS in the Martian magnetotail are in qualitative agreement with the model results. We may conclude that similarly to the Earth's magnetotail CS the quasi-adiabatic ion dynamics determines the structure and distribution of the current density in the Martian CS.

ACKNOWLEDGMENTS

We are grateful to O.L. Vaisberg for useful discussions and to the PIs and teams of the STATIC and MAG experiments for providing the data. The work was supported by the Russian Science Foundation (grant no. 16-42-01103).

REFERENCES

Acuña, M.H., Connerney, J.E.P., Ness, N.F., Lin, R.P., Mitchell, D., Carlson, C.W., McFadden, J., Anderson, K.A., Rème, H., Mazelle, C., Vignes, D., Wasilewski, P., and Cloutier, P., Global distribution of crustal magnetization discovered by the Mars Global Surveyor MAG/ER experiment, *Science*, 1999, vol. 284, pp. 790–793.

Büchner, J. and Zelenyi, L.M., Regular and chaotic charged particle motion in magnetotail-like field reversals: 1. Basic theory of trapped motion, *J. Geophys. Res.*, 1989, vol. 94, no. 10, pp. 11821–11842.

Connerney, J., Espley, J., Lawton, P., Murphy, S., Odom, J., Oliversen, R., and Sheppard, D., The MAVEN magnetic field investigation, *Space Sci. Rev.*, 2015, pp. 1–35. doi 10.1007/s11214-015-0169-4

Dubinin, E., Lundin, R., Riedler, W., Schwingenschuh, K., Luhmann, J.G., Russell, C.T., and Brace, L.H., Comparison of observed plasma and magnetic field structures in the wakes of Mars and Venus, *J. Geophys. Res.: Space Phys.*, 1991, vol. 96, pp. 11189–11197.

Eastwood, J.P., Phan, T.-D., Mozer, F.S., Shay, M.A., Fujimoto, M., Retinò, A., Hesse, M., Balogh, A., Lucek, E.A., and Dandouras, I., Multipoint observations of the hall electromagnetic field and secondary island formation during magnetic reconnection, *J. Geophys. Res.*, 2007, vol. 112, no. A06235. doi 10.1029/2006JA012158

Fairfield, D.H., On the average configuration of the geomagnetic tail, *J. Geophys. Res.*, 1979, vol. 84, p. 1950.

Ferguson, B.B., Cain, J.C., Crider, D.H., Brain, D.A., and Harnett, E.M., External fields on the night side of Mars at Mars Global Surveyor mapping altitudes, *Geophys. Res. Lett.*, 2005, vol. 32, no. L16105. doi 10.1029/2004GL021964

Grigorenko, E.E., Malova, H.V., Artemyev, A.V., Mingalev, O.V., Kronberg, E.A., Koleva, R., Daly, P.W., Cao, J.B., Sauvaud, J.-A., Owen, C.J., and Zelenyi, L.M., Current sheet structure and kinetic properties of plasma flows during a near-Earth magnetic reconnection under the presence of a guide field, *J. Geophys. Res.: Space Phys.*, 2013, vol. 118, pp. 3265–3287. doi 10.1002/jgra.50310

Grigorenko, E.E., Sauvaud, J.-A., Palin, L., Jacquey, C., and Zelenyi, L.M., THEMIS observations of the current sheet dynamics in response to the intrusion of the high-velocity plasma flow into the near-Earth magnetotail, *J. Geophys. Res.: Space Phys.*, 2014, vol. 119. doi 10.1002/2013JA019729

Grigorenko, E.E., Malova, H.V., Malykhin, A.Y., and Zelenyi, L.M., A possible mechanism of the enhancement and maintenance of the shear magnetic field component in the current sheet of the Earth's magnetotail, *Plasma Phys. Rep.*, 2015, vol. 41, no. 1, pp. 88–101.

Harada, Y., Halekas, J.S., McFadden, J.P., Mitchell, D.L., Mazelle, C., Connerney, J.E.P., Espley, J., Larson, D.E., Brain, D.A., Andersson, L., DiBraccio, G.A., Collinson, G.A., Livi, R., Hara, T., Ruhunusiri, S., and Jakosky, B.M., Magnetic reconnection in the near-Mars magnetotail: MAVEN observations, *Geophys. Res. Lett.*, 2015, vol. 42, pp. 8838–8845. doi 10.1002/2015GL065004

Jakosky, B.M., Lin, R.P., Grebowsky, J.M., Luhmann, J.G., Mitchell, D.F., Beutelschies, G., Priser, T., Acuna, M., Andersson, L., Baird, D., Baker, D., Bartlett, R., Benna, M., Bougher, S., Brain, D., et al., The Mars atmosphere and volatile evolution (MAVEN) mission, *Space Sci. Rev.*, 2015, vol. 195, pp. 3–48.

Kaumaz, Z., Siscoe, G.L., Luhmann, J.G., Lepping, R.P., and Russell, C.T., Interplanetary magnetic field control of magnetotail magnetic field geometry: IMP 8 observations, *J. Geophys. Res.: Space Phys.*, 1994, vol. 99, no. 6, p. 11113. doi 10.1029/94JA003000

Kronberg, E.A., Ashour-Abdalla, M., Dandouras, I., Delcourt, D.C., Grigorenko, E.E., Kistler, L.M., Kuzichev, I.V., Liao, J., Maggiolo, R., Malova, H.V., Orlova, K.G., Peroomian, V., Shklyar, D.R., Shprits, Y.Y., Welling, D.T., and Zelenyi, L.M., Circulation of heavy ions and their dynamical effects in the magnetosphere: recent observations and models, *Space Sci. Rev.*, 2014. doi 10.1007/s11214-014-0104-0

Malova, H., Popov, V.Yu., Mingalev, O.V., Mingalev, I.V., Mel'nik, M.N., Artemyev, A.V., Petrukovich, A.A., Delcourt, D.C., Shen, C., and Zelenyi, L.M., Thin current sheets in the presence of a guiding magnetic field in the Earth's magnetosphere, *J. Geophys. Res.: Space Phys.*, 2012, vol. 117, no. A04212. doi 10.1029/2011JA017359

Malova, H.V., Mingalev, O.V., Grigorenko, E.E., Mingalev, I.V., Melnik, M.N., Popov, V.Yu., Delcourt, D.C., Petrukovich, A.A., Shen, C., Rong, D., and Zelenyi, L.M., Formation of self-organized shear structures in thin current sheets, *J. Geophys. Res.: Space Phys.*, 2015, vol. 120. doi 10.1002/2014JA020974.2015

McFadden, J., Kortmann, O., Curtis, D., Dalton, G., Johnson, G., Abiad, R., Sterling, R., Hatch, K., Berg, P., Tiu, C., Gordon, D., Heavner, S., Robinson, M., Marckwordt, M., Lin, R., and Jakosky, B., MAVEN suprathermal and thermal ion composition (STATIC) instrument, *Space Sci. Rev.*, 2015, vol. 195, pp. 199–256.

Petrukovich, A.A., Artemyev, A.V., Malova, H.V., Popov, V.Yu., Nakamura, R., and Zelenyi, L.M., Embedded current sheets in the Earth's magnetotail, *J. Geophys.*

Res.: Space Phys., 2011, vol. 116, no. A00125. doi 10.1029/2010JA015749

Pritchett, P.L., Onset of magnetic reconnection in the presence of a normal magnetic field: realistic ion to electron mass ratio, *J. Geophys. Res.: Space Phys*., 2010, vol. 115, no. A10208. doi 10.1029/2010JA015371

Rong, Z.J., Wan, W.X., Shen, C., Li, X., Dunlop, M.W., Petrukovich, A.A., Zhang, T.L., and Lucek, E., Statistical survey on the magnetic structure in magnetotail current sheets, *J. Geophys. Res.: Space Phys*., 2011, vol. 116, no. A09218. doi 10.1029/2011JA016489

Runov, A., Nakamura, R., Baumjohann, W., Zhang, T.L., Volwerk, M., Eichelberger, H.-U., and Balogh, A., Cluster observation of a bifurcated current sheet, *Geophys. Res. Lett*., 2003, vol. 30, no. 2, p. 1036. doi 10.1029/2002GL016136

Slavin, J.A., Baker, D.N., Fairfield, D.H., Craven, J.D. Frank, L.A., Elphic, R.C., Galvin, A.B., Hughes, W.J., Manka, R.H., and Smith, E.J., CDAWEB 8 observations of plasmoid signatures in the geomagnetic tail: an assessment, *J. Geophys. Res.: Space Phys*., 1989, vol. 94, pp. 15153–15175. doi 10.1029/JA094iA11p15153

Sönnerup, B.U.Ö. and Scheible, M., Minimum and maximum variance analysis, in *Analysis Methods for Multi-Spacecraft Data*, Pashmann, G. and Daly, P.W., Eds., Bern: Int. Space Sci. Inst., 1998, chap. 8.

Zelenyi, L.M., Malova, H.V., Popov, V.Yu., Delcourt, D., and Sharma, A.S., Nonlinear equilibrium structure of thin currents sheets: influence of electron pressure anisotropy, *Nonlinear Process. Geophys*., 2004, vol. 11, no. 1, pp. 1–9.

Zelenyi, L.M., Malova, H.V., Popov, V.Y., Delcourt, D.C., Ganushkina, N.Y., and Sharma, A.S., "Matreshka" model of multilayered current sheet, *Geophys. Res. Lett*., 2006, vol. 33, art. ID L05105. doi 10.1029/2005GL025117

Zelenyi, L., Artemyev, A., Malova, H., and Popov, V., Marginal stability of thin current sheets in the Earth's magnetotail, *J. Atmos. Sol.-Terr. Phys*., 2008, vol. 70, pp. 325–333.

Zelenyi, L.M., Malova, Kh.V., Artemyev, A.V., Popov, V.Yu., and Petrukovich, A.A., Thin current sheets in collisionless plasma: equilibrium structure, plasma instabilities, and particle acceleration, *Plasma Phys. Rep*., 2011, vol. 37, no. 2, pp. 118–160.

Zelenyi, L.M., Malova, H.V., Grigorenko, E.E., and Popov, V.Yu., Thin current sheets: from the work of Ginzburg and Syrovatskii to the present day, *Phys.-Usp*., 2016, vol. 59, pp. 1057–1090.